Geoscientific
Model Development
Discussions

Open Access

Evaluation of an operational ocean model configuration at 1/12° spatial resolution for the Indonesian seas – Part 2: Biogeochemistry

E. Gutknecht[1], G. Reffray[1], M. Gehlen[2], I. Triyulianti[3], D. Berlianty[3], and P. Gaspar[4]

[1]Mercator Océan, 8–10 rue Hermès, 31520 Ramonville, France
[2]LSCE, UMR CEA-CNRS-UVSQ, Saclay, L'Orme des Merisiers, 91191 Gif-sur-Yvette, France
[3]Institute for Marine Research and Observation, Jl. Baru Perancak, Negara-Jembrana, Bali 82251, Republic of Indonesia
[4]CLS, 8–10 rue Hermès, 31520 Ramonville, France

Correspondence to: E. Gutknecht (elodie.gutknecht@mercator-ocean.fr)

Abstract

In the framework of the INDESO (Infrastructure evelopment of Space Oceanography) project, an operational ocean forecasting system was developed to monitor the state of the Indonesian seas in terms of circulation, biogeochemistry and fisheries. This forecasting system combines a suite of numerical models connecting physical and biogeochemical variables to population dynamics of large marine predators (tunas). The physical/biogeochemical coupled component (INDO12BIO configuration) covers a large region extending from the western Pacific Ocean to the Eastern Indian Ocean at 1/12° resolution. The OPA/NEMO physical ocean model and the PISCES biogeochemical model are coupled in "on-line" mode without degradation in space and time. The operational global ocean forecasting system (1/4°) operated by Mercator Ocean provides the physical forcing while climatological open boundary conditions are prescribed for the biogeochemistry.

This paper describes the skill assessment of the INDO12BIO configuration. Model skill is assessed by evaluating a reference hindcast simulation covering the last 8 years (2007–2014). Model results are compared to satellite, climatological and in situ observations. Diagnostics are performed on chlorophyll a, primary production, mesozooplankton, nutrients and oxygen.

Model results reproduce the main characteristics of biogeochemical tracer distributions in space and time. The seasonal cycle of chlorophyll a is in phase with satellite observations. The northern and southern parts of the archipelago present a distinct seasonal cycle, with higher chlorophyll biomass in the southern (northern) part during SE (NW) monsoon. Nutrient and oxygen concentrations are correctly reproduced in terms of horizontal and vertical distributions. The biogeochemical content of water masses entering in the archipelago as well as the water mass transformation across the archipelago conserves realistic vertical distribution in Banda Sea and at the exit of the archipelago.

1 Introduction

The "Coral triangle" delineated by Malaysia, the Philippines, New Guinea, Solomon Islands, East-Timor and Indonesia is recognized as a global hotspot of marine biodiversity (Allen and Werner, 2002; Mora et al., 2003; Green and Mous, 2004; Allen, 2008). It gathers 20 % of the world's species of plants and animals, and the greatest concentration and diversity of reefs (76 % of the world's coral species; Veron et al., 2009). The Indonesian archipelago is located at the centre of this ecologically rich region. It is characterized by a large diversity of coastal habitats such as mangrove forests, coral reefs and sea grass beds, all of which shelter ecosystems of exceptional diversity (Allen and Werner, 2002). The archipelago's natural heritage represents an important source of income and employment, with its future critically depending on the sustainable management of ecosystems and resources (e. g. Foale et al., 2013; Cros et al., 2014).

The wider Coral Triangle and its sub-region, the Indonesian archipelago, are facing multiple threats resulting from demographic growth, economic development, change in land use practices and associated deforestation, as well as global climate change (http://www.metoffice.gov.uk/media/pdf/8/f/Indonesia.pdf; FAO, 2007). Human activities cause changes in the delivery of sediments, nutrients and pollutants to coastal waters, leading to eutrophication, ecosystem degradation, as well as species extinctions (Ginsburg, 1994; Pimentel et al., 1995; Bryant et al., 1998; Roberts et al., 2002; UNEP, 2005; Alongi et al., 2013). Surveys report an over 30 % reduction of mangroves in Northern of Java over the last 150 years and an increase of coral reef degradation from 10 to 50 % in the last 50 years (Bryant et al., 1998; Hopley and Suharsono, 2000; UNEP, 2009), leading to 80 % of the reefs at risk in this region (Bryant et al., 1998). These changes not only damage coastal habitats, but propagate across the whole marine ecosystem from nutrients and the first levels of the food web up to higher trophic levels, along with concomitant changes in biogeochemical cycles.

E. Gutknecht et al.

There is thus a vital need for monitoring and forecasting marine ecosystem dynamics. The INDESO project (Infrastructure Development of Space Oceanography, www.indeso.web.id/indeso_wp/index.php), funded by the Indonesian Ministry of Marine Affairs and Fisheries, aims at the development of sustainable fishery practices in Indonesia, the monitoring of its Exclusive Economic Zone (EEZ) and the sustainable management of its ecosystems. The project addresses the Indonesian need for building a national capacity for operational oceanography. The model system consists of three models deployed at the scale of the Indonesian archipelago: an ocean circulation model (OPA/NEMO; Madec et al., 1998), a biogeochemical model (PISCES; Aumont and Bopp, 2006) and an intermediate trophic level/fish population dynamics model (SEAPODYM; Lehodey et al., 2008). Since mid-September 2014, the chain of models is fully operational in Perancak (Bali, Indonesia) and delivers 10 day forecast/two weeks hindcast on a weekly basis (see http://www.indeso.web.id).

The regional configuration of the physical model is based on the NEMO circulation model with a spatial resolution of 1/12°. The model is fully described in Tranchant et al. (this volume, hereafter Part 1). The comparison of model output to satellite, in situ and climatological data, as well as to previously published models demonstrated the skill of the model to correctly reproduce the main physical processes occurring in this complex oceanic region.

The present paper (Part 2) focuses on ocean biogeochemistry. It is organized as follows. The next section presents an overview of the area of study with emphasis on main forcings of biological production over the Indonesian archipelago. The biogeochemical component of the physical-biogeochemical coupled configuration (NEMO/PISCES) is described in Sect. 3. Satellite, climatological and in situ observations used to evaluate the simulation results are detailed in Sect. 4. Section 5 presents the evaluation of the skill of the coupled model to reproduce the main biogeochemical features of Indonesian seas along with their seasonal dynamics (Sect. 5). Finally, discussions and conclusions are presented in Sect. 6.

2 Area of study

The Indonesian archipelago is crossed by North and South Pacific waters that converge in the Banda Sea, and leave the archipelago through three main straits: Lombok, Ombaï and Timor. This ocean current (Indonesian ThroughFlow; ITF) provides the only low-latitude pathway for warm, fresh waters to move from the Pacific to the Indian Ocean (Gordon, 2005; Hirst and Godfrey, 1993). On their ways through the Indonesian archipelago, water masses are progressively transformed by surface heat and freshwater fluxes and intense vertical mixing linked to strong internal tides trapped in the semi-enclosed seas as well as upwelling processes (Ffield and Gordon, 1992). The main flow, as well as the transformation of Pacific waters is correctly reproduced by the physical model, with a realistic distribution of the volume transport through the three major outflow passages (Part 1). In the Indian Ocean, this thermocline water mass forms a cold and fresh tongue between 10 and 20° S, and supplies the Indian Ocean in nutrients. These are likely to impact biogeochemical cycles and support new primary production in the Indian Ocean (Ayers et al., 2014).

Over the archipelago, complex meteorological and oceanographic conditions drive the distribution and growth of phytoplankton and provide favourable conditions for the development of a diverse and productive food web extending from zooplankton, and intermediate trophic levels to pelagic fish (Hendiarti et al., 2004, 2005; Romero et al., 2009). The tropical climate is characterized by a monsoon regime and displays a well-marked seasonality. The south-east (SE) monsoon (April to October) is associated with easterlies from Australia that carry warm and dry air over the region. Wind-induced upwelling along the southern coasts of Sumatra, Java and Nusa–Tenggara Islands (hereafter named Sunda Islands) and in the Banda Sea is associated with high chlorophyll *a* levels (Susanto et al., 2006; Rixen et al., 2006). Chlorophyll *a* maxima along Sunda Islands move to the west over the period of the SE monsoon, in response to the alongshore wind shift and associated movement of the upwelling centre (Susanto et al., 2006). From October to April, the northwest (NW) monsoon is associated with warm

Full Screen / Esc

and moist winds from the Asian continent. Winds blow in a southwest direction north of the Equator and towards Australia south of the Equator. They generate a downwelling and a reduced chlorophyll *a* content south of the Sunda Islands and in the Banda Sea. The NW monsoon also causes some of the highest precipitation rates in the world.
5 Increased river runoff carries important sediment loads (20 to 25 % of the global riverine sediment discharge; Milliman et al., 1999), along with carbon and nutrients to the ocean. These inputs are a strong driver of chlorophyll *a* variability and play a key role in modulating the biological carbon pump across Indonesian seas (Hendiarti et al., 2004; Rixen et al., 2006). High levels of suspended matter decrease the water transparency
10 in the coastal areas and modify the optical properties of waters which in turn interferes ocean colour remote sensing (Susanto et al., 2006). Although several Indonesian rivers are classified among the 100 most important rivers of the world, most of them are not regularly monitored. It is thus currently impossible to estimate the impact of river runoff on chlorophyll *a* variability in the region (Susanto et al., 2006).
15 In addition to the seasonal variability driven by the Asia–Australia monsoon system, Indonesian seas are influenced by the El Niño Southern Oscillation (ENSO) which modulates rainfall and chlorophyll *a* on inter-annual timescales (Susanto et al., 2001, 2006; Susanto and Marra, 2005). Other forcing such as tides, the Madden–Julian Oscillation, Kelvin and Rossby waves, and the Indian Ocean Dipole also affect the Indone-
20 sian seas and influence the marine ecosystems (Madden and Julian, 1994; Ffield and Gordon, 1996; Sprintall et al., 2000; Susanto et al., 2000, 2006).

3 The INDO12BIO configuration

In the framework of the INDESO project, a coupled physical-biogeochemical model is deployed over the domain from 90–144° E to 20° S–25° N, widely encompassing the
25 whole Indonesian archipelago. The physical model is based on the OPA (NEMO2.3) circulation model (Madec et al., 1998; Madec, 2008). Specific improvements include time-splitting and non-linear free surface to correctly simulate high frequency processes

such as tides. The physical configuration is called INDO12. It is described in detail in Part 1 (Tranchant et al., 2015). Biogeochemical dynamics of the area are simulated by the PISCES model, version 3.2 (Aumont and Bopp, 2006). PISCES simulates the first levels of the marine food web from nutrients up to mesozooplankton. It has 24 state variables. PISCES considers five limiting nutrients for phytoplankton growth (nitrate, ammonium, phosphate, dissolved Si and iron). Four living size-classified compartments are represented: two phytoplankton groups (nanophytoplankton and diatoms), and two zooplankton groups (microzooplankton and mesozooplankton). The model includes five non-living compartments: small and big particulate organic carbon and semi-labile dissolved organic carbon, particulate inorganic carbon ($CaCO_3$ or calcite) and biogenic silica. For phytoplankton compartments, total biomass in C, Fe, Si (for diatoms) and chlorophyll and hence the internal Fe/C, Chl/C, and Si/C ratios are prognostically simulated. For zooplankton, only the total biomass in carbon is a prognostic variable. PISCES simulates Dissolved Inorganic Carbon (DIC), total alkalinity (carbonate alkalinity + borate + water), and dissolved oxygen. The CO_2 chemistry is computed following the OCMIP protocols (http://ocmip5.ipsl.jussieu.fr/OCMIP/). Biogeochemical parameters are based on PISCES namelist version 3.2.

Physical and biogeochemical model components are coupled on-line without degradation in space and time. The coupled configuration is called INDO12BIO and its specifications are detailed hereafter.

3.1 Numerical aspects

PISCES is coupled online to the physical component and attention must be paid to respect a number of fundamental numerical constraints. (1) The numerical scheme of PISCES for biogeochemical processes is forward in time (Euler), which does not correspond to the classical leap-frog scheme used for the physical component. Moreover, the free surface explicitly solved by the time splitting method is non linear. In order to respect the conservation of the tracers, the coupling between biogeochemical and physical components is done one time step over two. As a result, the biogeochemical

model is controlled by only one leap-frog trajectory of the dynamical model. The use of an asselin filter allows to keep the two numerical trajectories close enough to overcome this shortcoming. The advantage is a reduction of numerical cost and a time step for the biogeochemical model twice that of the physical component ie. 900 s. (2) As this time step is small, no time-splitting was used in the sedimentation scheme. (3) The advection scheme is the standard scheme of TOP-PISCES ie. the Monotonic Upstream centered Scheme for Conservation Laws (MUSCL) (Van Leer, 1977). No explicit diffusion has been added as the numerical diffusion introduced by this advection scheme is already important.

3.2 Initial and open boundary conditions

The simulation starts on 3 January 2007 from the global ocean forecasting system at 1/4° operated by Mercator Ocean (PSY3 described in Lellouche et al., 2013) for temperature, salinity, currents, and free surface at the same date. Open boundary conditions (OBC) are also provided by daily outputs of this system. A 1° thick buffer layer allows nudging the signal at the open boundaries.

Initial and open boundary conditions are derived from climatological data bases for nitrate, phosphate, dissolved Si, oxygen, dissolved inorganic carbon, and alkalinity. For tracers for which this information is missing, initial and open boundary conditions come either from global models, or have to be estimated from satellite data, respectively build using analytical values. Initial and open boundary conditions are presented in Table 1. A Dirichlet boundary condition is used to improve the information exchange between the OBC and the interior of the domain.

3.3 External inputs

The model considers two external Fe sources: (1) atmospheric dust deposition from the monthly climatology of Aumont et al. (2003), and (2) sedimentary Fe supply (Aumont and Bopp, 2006). Yearly nutrient and carbon fluxes from river discharge are provided

by Ludwig et al. (1996) and Global News 2 (Mayorga et al., 2010) climatologies. In PISCES, global external input fluxes are compensated by a loss to the sediments as particulate organic matter, biogenic Si and $CaCO_3$. These fluxes correspond to matter definitely lost from the ocean system. The compensation of external input fluxes through output at the lower boundary closes the mass balance of the model. While this equilibrium is a valid assumption at the scale of the global ocean, it is not established at regional scale. For the INDO12BIO configuration, a decrease of the nutrient and carbon loss to the sediment was introduced corresponding to an increase in the water column remineralization by $\sim 4\%$. This slight enhancement of water column remineralization leads to higher coastal chlorophyll a concentrations (about $+1\,\mathrm{mg\,Chl\,m^{-3}}$) and enables the model to reproduce the chlorophyll a maxima observed along the coasts of Australia and East Sumatra (not shown).

3.4 Simulation length

The simulation started on 3 January 2007 and operates up to present day as the model currently delivers ocean forecasts. The spin-up length depends on the biogeochemical tracer (Fig. 1). The total carbon inventory computed over the domain (defined as the sum of all solid and dissolved organic and inorganic carbon fractions, yet dominated by the contribution of DIC) equilibrates within several months. To the contrary, Dissolved Organic Carbon (DOC), phosphate (PO_4) and Iron (Fe) need several years to stabilize (Fig. 1). The annual and seasonal validation presented in the following focuses on years 2010 to 2014.

4 Satellite, climatological and in situ data

Model output is compared to satellite, climatological, and in situ observations. These observational data are detailed and described in this section.

4.1 Chlorophyll *a*

The ocean colour signal reflects a combination of chlorophyll *a* content, suspended matter, coloured dissolved organic matter (CDOM) and bottom reflectance. Singling out the contribution of phytoplankton's chlorophyll *a* is not straightforward in waters for which the relative optical contribution of the three last components is significant. This is the case over vast areas of the Indonesian archipelago where river discharges and shallow water depths contribute to optical properties (Susanto et al., 2006). The interference with optically absorbing constituents other than chlorophyll *a* results in large uncertainties in coastal waters (up to 100 %, as compared to 30 % for open ocean waters) (Moore et al., 2009). Standard algorithms distinguish between open ocean waters/clear waters (Case 1) and coastal waters/turbid waters (Case 2). The area of deployment of the model comprises waters of both categories and the comparison between modelled chlorophyll *a* and estimates derived from remote sensing can be only qualitative. Two single mission monthly satellite products are used for model skill evaluation. MODIS-Aqua (EOS mission, NASA) Level 3 Standard Mapped Image product (NASA Reprocessing 2013.1) covers the whole simulated period (2007–2014). It is a product for Case 1 waters, with a 9 km resolution, and is distributed by the ocean colour project (http://oceancolor.gsfc.nasa.gov/cms/). The MERIS (ENVISAT, ESA) L3 product (ESA 3rd reprocessing 2011) is also considered. Its spectral characteristics allow the use of an algorithm for Case 2 waters (MERIS C2R Neural Network algorithm; Doerffer and Schiller, 2007). It has a 4 km resolution and is distributed by ACRI.-ST, unfortunately the mission ended in April 2012.

4.2 Net primary production

Net primary production (NPP) is at the base of the food-chain. In situ measurements of primary production are sparse and we rely on products derived from remote sensing for model evaluation. The link between pigment concentration (chlorophyll *a*) and carbon assimilation reflects the distribution of chlorophyll *a* concentrations, but also

the uncertainty associated to the production algorithm and the ocean colour prod-uct. At present, three production models are used by the community. The Vertically Generalized Production Model (VGPM) (Behrenfeld and Falkowski, 1997) estimates NPP as a function of chlorophyll, available light, and the photosynthetic efficiency. It is currently considered as the Standard algorithm. The two alternative algorithms are an "Eppley" version of the VGPM (distinct temperature-dependent description of pho-tosynthetic efficiencies) and the Carbon-based Production Model (CbPM; Behrenfeld et al., 2005; Westberry et al., 2008). The latter estimates phytoplankton carbon concen-tration from remote sensing particulate scattering coefficients. A complete description of the products is available at www.science.oregonstate.edu/ocean.productivity. Here we compare the simulated NPP to NPP derived from the three production models using MODIS ocean colour estimates.

4.3 Mesozooplankton

The MARine Ecosystem DATa (MAREDAT) is a collection of global biomass datasets containing the major plankton functional types (e. g. diatoms, microzooplankton, meso-zooplankton . . .). Mesozooplankton is the only MAREDAT field covering the Indonesian archipelago. The database provides monthly fields at a spatial resolution of 1°. Meso-zooplankton data are described in Moriaty and O'Brien (2013). Samples are taken with a single net towed over a fixed depth interval (e. g. 0–50, 0–100, 0–150, 0–200 m . . .) and represent the average population biomass ($\mu g\,C\,L^{-1}$) throughout a depth interval. For this study, only annual mean mesozooplankton biomasses are used. Monthly fields have a too sparse spatial coverage over the Indonesian archipelago and represent different years. It is thus not possible to extract a seasonal cycle.

4.4 Nutrients and oxygen

Modelled nutrient and oxygen distributions are compared to climatological fields of World Ocean Atlas 2009 (WOA 2009, 1° spatial resolution) (Garcia et al., 2010a, b),

respectively, the CSIRO Atlas of Regional Seas 2009 (CARS 2009, 0.5° spatial resolution) and discreet observations provided by the World Ocean Database 2009 (WOD 2009) Only nitrate, dissolved Si and oxygen distributions are presented hereafter. Nitrate + ammonium and phosphate are linked by a Redfield ratio in PISCES.

4.5 INDOMIX cruise

The INDOMIX cruise on-board RV *Marion Dufresne* (Koch-Larrouy et al., 2015) crossed the Indonesian archipelago between the 9 and 19 July 2010, and focused on one of the most energetic sections for internal tides from Halmahera Sea to Ombaï Strait. Repeated CTD profiles over 24 h as well as measurements of oxygen and nutrients were obtained for six stations at the entrance of the archipelago (Halmahera Sea), in the Banda Sea and in the Ombaï Strait (three of them are use for validation; cf stations on Fig. 2). This data set provides an independent assessment of model skill. To co-localise model and observations, we took the closest simulated point to the coordinates of the station. 2 day model averages were regarded as measurements were performed during 2 consecutive days at the stations selected for validation.

5 INDO12BIO evaluation

The ability of the INDO12BIO coupled physical-biogeochemical model to reproduce the observed spatial distribution and temporal variability of biogeochemical tracers is assessed for chlorophyll *a*, net primary production, mesozooplankton biomass, nutrients and oxygen concentrations. Model evaluation focuses on the annual mean state and the seasonal cycle based on the period 2010 to 2014.

5.1 Annual mean state Chlorophyll *a*, NPP and mesozooplankton biomass

The simulation reproduces the main characteristics of the large scale distribution of chlorophyll *a*, a proxy of phytoplankton biomass (Fig. 2). Pacific and Indian subtrop-

ical gyres are characterized by low concentrations due to gyre-scale downwelling and hence a deeper nutricline. Highest concentrations are simulated along the coasts driven by river nutrient supply and upwelling of nutrient-rich deep waters. In comparison to the Case 1 ocean colour product, the model overestimates the chlorophyll *a*

5   content of oligotrophic gyres and the cross-shore gradient is too weak. As mentioned in the preceding section, optical characteristics of waters of the Indonesian archipelago are closer to Case 2 waters (Moore et al., 2009). As a matter of fact, simulated chlorophyll *a* concentrations are closer to those derived with an algorithm for Case 2 waters (MERIS).

10   The model correctly reproduces the spatial distribution, as well the rates of NPP over the model domain (Fig. 3). However, as mentioned before, NPP estimates depend on the primary production model (in this case, VGPM, CbPM, and Eppley) and on the ocean colour data used in the production models. For a single ocean colour product (here MODIS), NPP estimates display a large variability (Fig. 3). NPP estimates from

15   VGPM are characterized by low rates in the Pacific ($< 10\,\mathrm{mmol\,C\,m^{-2}\,d^{-1}}$) and a well marked cross-shore gradient. The use of CbPM results in low coastal NPP and almost uniform rates over a major part of the domain and including the open ocean (Fig. 3). The Eppley production model is the most productive one with rates about $15\,\mathrm{mmol\,C\,m^{-2}\,d^{-1}}$ in the Pacific and higher than $300\,\mathrm{mmol\,C\,m^{-2}\,d^{-1}}$ in the coastal

20   zone. The large uncertainty associated with these products precludes a quantitative evaluation of modelled NPP. Like for chlorophyll *a*, modelled NPP falls within the range of remote sensing derived estimates, with maybe a too weak cross-shore gradient inherited from the chlorophyll *a* field.

   Mesozooplankton link the first level of the marine food web (primary producers) to

25   the mid- and, ultimately, high trophic levels. Modelled mesozooplankton biomass is compared to observations in Fig. 4. While the model reproduces the spatial distribution of mesozooplankton, it overestimates biomass by a factor 2 or 3. This overestimation is likely linked to the above-described overestimation of the phytoplankton biomass.

Full Screen / Esc

Printer-friendly Version

Interactive Discussion

5.2 Annual mean state nutrients and oxygen

Nitrate and oxygen distributions at 100 m depth are presented on Fig. 5 for CARS, WOA and the model. Dissolved Si has the same distribution as nitrate (not shown on Fig. 5). The marked meridional gradient present in observations of the Pacific and Indian Oceans is correctly reproduced by the model (Fig. 5). Low nitrate and high oxygen concentrations in the subtropical gyres of the North Pacific and South Indian Oceans are due to Ekman-induced downwelling. Higher nitrate and lower oxygen concentrations in the equatorial area are associated with upwelling process. Maxima nitrate concentrations associated with minima oxygen concentrations are noticeable in the Bay of Bengal and Adaman Sea (north of Sumatra and west of Myanmar; Fig. 5). They reflect discharges by major rivers (Brahmaputra, Ganges and other river systems) and associated increase in oxygen demand. Low nitrate and high oxygen concentrations at 100 m depth in the Sulawesi Sea reflect the signature of Pacific waters entering in the archipelago, a feature correctly reproduced by the model. The signature slowly disappears as waters progressively mix along their pathways across the archipelago. The resulting higher nitrate and lower oxygen levels at 100 m depth in the Banda Sea are captured by the model. Higher nitrate and oxygen concentrations off the Java–Nusa–Tenggara island chain in data and model output reflect seasonal alongshore upwelling.

To evaluate the vertical distribution of simulated nutrient and oxygen concentrations over the Indonesian archipelago, vertical profiles of oxygen, nitrate and dissolved Si are compared to climatologies provided by CARS and WOA, as well as to discreet data from WOD (Fig. 6). Vertical profiles are analysed in key areas for the Indonesian ThroughFlow (Koch-Larrouy et al., 2007): (1) one box in the North Pacific Ocean, which is representative of water masses entering the archipelago, (2) one box in the Banda Sea where Pacific waters are mixed to form the ITF, and (3) one box at the exit of the Indonesian archipelago (Timor Strait). Biogeochemical characteristics of tropical Pacific water masses entering the archipelago are correctly reproduced by the model (Fig. 6). The flow across the Indonesian archipelago and the transformation of water

Title Page

Abstract | Introduction

Conclusions | References

Tables | Figures

◀ | ▶

◀ | ▶

Back | Close

Full Screen / Esc

Printer-friendly Version

Interactive Discussion

masses simulated by the model result in realistic vertical distributions of nutrients and oxygen concentrations in the Banda Sea. The ITF leaves the archipelago and spreads into the Indian Ocean with a biogeochemical content in good agreement with the data available in the area.

However, the modelled vertical structures are too smooth. The vertical gradient of nitrate is too weak over the first 1500 m depth of the water column (see North Pacific box on Fig. 6). This bias is even more pronounced on vertical gradient of dissolved Si (Fig. 6). These sluggish vertical structures result from the numerical advection scheme MUSCL currently used in PISCES which is known to be too diffusive (Lévy et al., 2001).

5.3 Seasonal cycle

The monsoon system drives the seasonal variability of chlorophyll *a* over the area of study. Northern and southern parts of the archipelago exhibit a distinct seasonal cycle (Fig. 7). In the southern part, the highest chlorophyll concentrations occur from June to September (Fig. 7) due to upwelling of nutrient-rich waters off Sunda Islands and in the Banda Sea triggered by alongshore south-easterly winds during SE monsoon. The decrease in chlorophyll levels during NW monsoon is the consequence of north-westerly winds and associated downwelling in these same areas. In the northern part, high chlorophyll concentrations occur during NW monsoon (Fig. 7) when moist winds from Asia cause intense precipitations. A secondary peak is observed during NW monsoon in the southern part and during SE monsoon in the northern part due to meteorological and oceanographic conditions described above.

The annual signal of chlorophyll *a* in each grid point gives a synoptic view of the effect of the Asia–Australia monsoon system on the Indonesian archipelago. A harmonic analysis is applied on the time series of each grid point to extract the annual signal in model output and remote sensing data (MODIS). The results of the annual harmonic analysis are summarized in Fig. 8 and highlight the month of the maximum phase and the amplitude of the annual signal. The phase of the modelled chlorophyll *a* concentration presents a north–south distribution in agreement with the satellite observations.

The simulation reproduces the chlorophyll *a* maxima in July in the Banda Sea and off the south coasts of Java–Nusa–Tenggara. Consistent with observations, simulated chlorophyll *a* maxima move to the west over the period of the SE monsoon, in response to the alongshore wind shift. North of the Nusa–Tenggara Islands, maxima in January–February are due to upwelling associated with alongshore north-westerly winds. In the South China Sea, maxima spread from July–August in the western part (off Mekong River) and gradually shift up to January–February in the eastern part. The temporal correlation between modelled chlorophyll *a* and estimates derived from remote sensing exceeds 0.7 in the South-East China sea, the Banda Sea and in the Indian Ocean (Fig. 9). This high correlation coefficient is associated with low normalized standard deviations (close to 1) in the Banda Sea and in the Indian Ocean (Fig. 9) and large amplitudes in simulated and observed chlorophyll *a* (Fig. 8). Normalized standard deviations are higher in the South-East China Sea, Java and Flores Seas, but also in the open ocean due to larger amplitudes in simulated chlorophyll *a*. The offshore spread of the high amplitude reflects the too weak cross-shore gradient of simulated chlorophyll *a* (Sect. 5.1), and leads to an increase of the normalized standard deviation with the distance to the coast. For semi-enclosed seas (South-East China Sea, Java and Flores Seas), however, this result has to be taken with caution as clouds cover these regions almost 50–60 % of the time period.

The model does not succeed in simulating chlorophyll *a* variability in the Pacific sector (Figs. 8 and 9). This area is close to the border of the modelled domain and is influenced by the OBCs derived from the global operational ocean general circulation model. Analysis of the modelled circulation (Part 1) highlights the role of OBCs in maintaining realistic circulation patterns in this area, which is influenced by the equatorial current system. Part 1 points, in particular, to the incorrect positioning of Halmahera and Mindanao eddies in the current model, which contributes to biases in simulated biogeochemical fields.

Finally, correlation is low close to the coasts and the temporal variability of the model is lower than that of the satellite product, with normalized standard deviation < 1

(Fig. 9). The model does not take into account seasonal nutrient input from rivers driven by the monsoon system. These external sources of nutrients impact chlorophyll *a* variability at local scale.

5.4 INDOMIX cruise

Model results are compared to INDOMIX in situ data at three key locations: (1) the eastern entrance of Pacific waters to the archipelago (station 3, Halmahera Sea), (2) the convergence of the western and eastern pathways (station 4, Banda Sea) where intense tidal mixing and upwelling transforms Pacific waters to form the ITF, and (3) one of the main exit portals of the ITF to the Indian Ocean (station 5, Ombaï Strait).

The vertical profile of temperature compares well with the data in the Halmahera Sea (Fig. 10). Simulated surface waters are too salty and the subsurface salinity maximum is reproduced at the observed depth, albeit underestimated compared to the data. Waters are more oxygenated in the model over the first 400 m. The model-data bias on temperature, salinity and oxygen suggests that thermocline waters are not correctly reproduced by the model at the Halmahera Sea in July 2010. The model tends to yield too smooth vertical profiles. Vertical profiles of nitrate and phosphate are pretty well reproduced, while dissolved Si concentrations are overestimated below 200 m depth. Different mechanisms could explain this difference such as a silicate-based process not solved in the biogeochemical model, or a too strong external input of dissolved Si in the model. However, the property of dissolved Si as tracer for water masses confirms the weakness of the model to reproduce realistic water masses in Halmahera Sea (Part 1).

Despite the failing evaluation in Halmahera sea, an overall satisfying correspondence between modelled and observed profiles is found at the Banda Sea (Fig. 11) and Ombaï Strait stations (Fig. 12). The comparison of modelled profiles and cruise data along the flow path of waters from the Pacific to the Indian Ocean (from Halmahera to Ombaï Strait) suggests that either the Halmahera Sea had no major influence for the ITF formation during the time of the cruise, or that vertical mixing and upwelling processes

across the archipelago are strong enough to allow the formation of Indonesian water masses despite biases in source water composition.

6   Discussions and conclusions

The INDO12BIO coupled physical-biogeochemical simulation was evaluated against satellite, climatological and in situ datasets for years 2010 to 2014. Model skill was assessed focussing on chlorophyll *a*, primary production, mesozooplankton, nutrient and oxygen concentrations.

The model reproduces the main characteristics of the large scale distribution of chlorophyll *a* concentrations, depth integrated NPP rates and mesozooplankton biomass. The simulated seasonal cycle of chlorophyll *a* concentration is in phase with satellite-based estimations. The northern and southern parts of the archipelago present a distinct seasonal cycle, with higher chlorophyll biomass in the southern part during SE monsoon, and in the northern part of the archipelago during NW monsoon.

Horizontal and vertical distributions of nutrients and oxygen concentrations are correctly reproduced by the model. Annual mean biogeochemical characteristics of tropical North Pacific water masses entering in the archipelago are correctly simulated by the coupled model. Transformation of water masses overs the Indonesian archipelago is correctly simulated with modelled concentrations of nitrate and oxygen in the Banda Sea and at the exit of the archipelago close to observations.

Chlorophyll *a* concentrations in coastal waters are influenced by riverine nutrient input and sedimentary processes (i. e. remineralization of organic carbon and subsequent release of nutrients). The slight disequilibrium introduced between the external input of nutrients and carbon and the loss to the sediment is sufficient to enhance chlorophyll *a* concentrations along the coasts in line with observations. The sensitivity of the model to the balancing of carbon and nutrients at the lower boundary of the domain ("sediment burial") highlights the need for an explicit representation of sedimentary reactions. The improved representation of the seasonal cycle of chlorophyll *a*

in coastal regions further calls for the consideration of seasonality in river nutrient and carbon inputs. According to Jennerjahn et al. (2004), river discharges from Java can be increased by a factor of ∼ 12 during NW monsoon as compared to SE monsoon. Moreover the maximum fresh water transport and the peak of material reaching the sea can

5   be out of phase depending on the origin of discharged material (Hendiarti et al., 2004). The improved representation of river discharge dynamics and associated delivery of fresh water, nutrients and suspended matter is, however, hampered by the availability of data. As a matter of fact, most of the Indonesian rivers are currently not monitored (Susanto et al., 2006).

10   Systematic misfits between modelled and observed biogeochemical distributions may also reflect inherent properties of implemented numerical schemes. Misfits highlighted throughout this work include too weak cross-shore gradients of modelled chlorophyll a, and NPP (coast to open ocean) together with noticeable smoothing of vertical profiles of modelled properties. Currently, the MUSCL advection scheme is used for

15   biogeochemical tracers. This scheme is too diffusive and smooths vertical profiles of biogeochemical tracers. As a result, too much nutrients are injected in the surface layer and trigger high levels of chlorophyll a and NPP. Another advection scheme, QUICKEST (Leonard, 1979) with the limiter of Zalezak (1979), already used in NEMO for the advection scheme of the physical model, has been tested for biogeochemical trac-

20   ers. Switching from MUSCL to QUICKEST-Zalezak accentuates the vertical gradient of nutrients in the water column and attenuates modelled chlorophyll a and NPP. This advection scheme is not diffusive and coherent with model physics. But his use stresses too much the vertical gradient of nutrients, highlighting the need to improve the model physics. Indeed, neither tuning of biogeochemical parameters, nor switching the ad-

25   vection scheme for passive tracers fully resolved the model-data misfits. Improving the vertical distribution of nutrients and oxygen, as well as chlorophyll a levels and NPP in the open ocean and their cross-shore gradient relies at first order on the model physics.

Finally, monthly or yearly climatologies are currently used for initial and open boundary conditions. These biogeochemical tracers are thus decorrelated from model

physics. In order to improve the link between modelled physics and biogeochemistry, weekly or monthly averaged output of the operational system operated by Mercator Ocean (BIOMER4) will be used in the future for the 24 tracers of the biogeochemical model PISCES. BIOMER4 couples the physical forecasting system PSY3 to PISCES in off-line mode. The biogeochemical and the physical components of INDOBIO12 will thus be initialized and forced by the same PSY3 forecasting system.

References

Allen, G. R.: Conservation hotspots of biodiversity and endemism for Indo-Pacific coral reef fishes, Aquat. Conserv., 18, 541–556, doi:10.1002/aqc.880, 2008.

Allen, G. R. and Werner, T. B.: Coral Reef Fish Assessment in the "Coral Triangle" of Southeastern Asia, Environ. Biol. Fish., 65, 209–2014, doi:10.1023/A:1020093012502, 2002.

Alongi, D. A., da Silva, M., Wasson, R. J., and Wirasantosa, S.: Sediment discharge and export of fluvial carbon and nutrients into the Arafura and Timor Seas: a regional synthesis, Mar. Geol., 343, 146–158, doi:10.1016/j.margeo.2013.07.004, 2013.

Aumont, O. and Bopp, L.: Globalizing results from ocean in situ iron fertilization studies, Global Biogeochem. Cy., 20, GB2017, doi:10.1029/2005GB002591, 2006.

Aumont, O., Maier-Reimer, E., Blain, S., and Monfray, P.: An ecosystem model of the global ocean including Fe, Si, P colimitations, Global Biogeochem. Cy., 17, 1060, doi:10.1029/2001GB001745, 2003.

Ayers, J. M., Strutton, P. G., Coles, V. J., Hood, R. R., and Matear, R. J.: Indonesian throughflow nutrient fluxes and their potential impact on Indian Ocean productivity, Geophys. Res. Lett., 41, 5060–5067, doi:10.1002/2014GL060593, 2014.

Behrenfeld, M. J. and Falkowski, P. G.: Photosynthetic rates derived from satellite-based chloro-phyll concentration, Limnol. Oceanogr., 42, 1–20, 1997.

Behrenfeld, M. J., Boss, E., Siegel, D. A., and Shea, D. M.: Carbon-based ocean produc-tivity and phytoplankton physiology from space, Global Biogeochem. Cy., 19, GB1006, doi:10.1029/2004GB002299, 2005.

Bryant, D., Burke, L., McManus, J., and Spalding, M.: Reefs at Risk: a Map-Based Indicator of Potential Threats to the World's Coral Reefs, World Resources Institute, Washington, DC; International Center for Living Aquatic Resource Management, Manila; and United Nations Environment Programme World Conservation Monitoring Centre, Cambridge, 1998.

Cros, A., Fatan, N. A. White, A., Teoh, S. J., Tan, S., Handayani, C., Huang, C., Peterson, N., Li, R. V., Siry, H. Y., Fitriana, R., Gove, J., Acoba, T., Knight, M., Acosta, R., Andrew, N., and Beare, D.: The Coral Triangle Atlas: an integrated online spatial database system for im-proving coral reef management, PLoS ONE, 9, e96332, doi:10.1371/journal.pone.0096332, 2014.

CSIRO: Atlas of Regional Seas, available at: http://www.marine.csiro.au/~dunn/cars2009/ (last access: 13 August 2015), 2009.

Doerffer, R. and Schiller, H: The MERIS Case 2 water algorithm, Int. J. Remote Sens., 28, 517–535, doi:10.1080/01431160600821127, 2007.

FAO: United Nations Food and Agricultural Organization, FAOSTAT, available at: http://faostat.fao.org/site/291/default.aspx (last access: 13 August 2015), 2007.

Ffield, A. and Gordon, A. L.: Vertical mixing in the Indonesian thermocline, J. Phys. Oceanogr., 22, 184–195, 1992.

Ffield, A. and Gordon, A. L.: Tidal mixing signatures in the Indonesian seas, J. Phys. Oceanogr., 26, 1924–1937, 1996.

Foale, S., Adhuri, D., Aliño, P., Allison, E. H., Andrew, N., Cohen, P., Evans, L., Fabinyi, M., Fidelman, P., Gregory, C., Stacey, N., Tanzer, J., and Weeratunge, N.: Food security and the Coral Triangle Initiative, Mar. Policy, 38, 174–183, doi:10.1016/j.marpol.2012.05.033, 2013.

Garcia, H. E., Locarnini, R. A., Boyer, T. P., Antonov, J. I., Baranova, O. K., Zweng, M. M., and Johnson, D. R.: World Ocean Atlas 2009, Volume 3 Dissolved Oxygen, Apparent Oxygen Utilization, and Oxygen Saturation, edited by: Levitus, S., NOAA Atlas NESDIS 70, U.S. Government Printing Office, Washington, D.C., 344 pp., 2010a.

Garcia, H. E., Locarnini, R. A., Boyer, T. P., Antonov, J. I., Zweng, M. M., Baranova, O. K., and Johnson, D. R.: World Ocean Atlas 2009, Volume 4 Nutrients (phosphate, nitrate, silicate),

Evaluation of an operational ocean model for the Indonesian seas – Part 2

E. Gutknecht et al.

edited by: Levitus, S., NOAA Atlas NESDIS 71, U.S. Government Printing Office, Washington, D.C., 398 pp., 2010b.

Ginsburg, R. N. (Ed.): Proceedings of the Colloquium on Global Aspects of Coral Reefs: Health, Hazards and History, Atlantic Reef Committee, 1994.

Gordon, A. L.: Oceanography of the Indonesian seas and their throughflow, Oceanography, 18, 14–27, doi:10.5670/oceanog.2005.01, 2005.

Green, A. and Mous, P. J.: Delineating the Coral Triangle, its ecoregions and functional seascapes, Report on an expert workshop held in Southeast Asia Center for Marine Protected Areas, Bali, Indonesia, 30 April–2 May 2003, The Nature Conservancy, 2004.

Hendiarti, N., Siegel, H., and Ohde, T.: Investigation of different coastal processes in Indonesian waters using SeaWiFS data, Deep-Sea Res. Pt. II, 51, 85–97, doi:10.1016/j.dsr2.2003.10.003, 2004.

Hendiarti, N., Suwarso, E., Aldrian, E., Amri, K., Andiastuti, R., Sachoemar, S. I., and Wahyono, I. B.: Seasonal variation of pelagic fish catch around Java, Oceanography, 18, 112–123, doi:10.5670/oceanog.2005.12, 2005.

Hirst, A. C. and Godfrey, J. S.: The role of Indonesian throughflow in a global ocean GCM, J. Phys. Oceanogr., 23, 1057–1086, 1993.

Hopley, D. and Suharsono, M.: The Status of Coral Reefs in Eastern Indonesia, Australian Institute of Marine Science, Townsville, Australia, 2000.

Jennerjahn, T. C., Ittekkot, V., Klopper, S., Adi, S., Purwo Nugroho, S., Sudiana, N., Yusmal, A., and Gaye-Haake, B.: Biogeochemistry of a tropical river affected by human activities in its catchment: Brantas River estuary and coastal waters of Madura Strait, Java, Indonesia, Estuar. Coast. Shelf S., 60, 503–514, doi:10.1016/j.ecss.2004.02.008, 2004.

Key, R. M., Kozyr, A., Sabine, C. L., Lee, K., Wanninkhof, R., Bullister, J., Feely, R. A., Millero, F., Mordy, C., and Peng, T.-H.: A global ocean carbon climatology: Results from GLODAP, Global Biogeochemical Cycles, Vol. 18, GB4031, doi:10.1029/2004GB002247, 2004.

Koch-Larrouy, A., Madec, G., Bouruet-Aubertot, P., Gerkema, T., Bessieres, L., and Molcard, R.: On the transformation of Pacific water into Indonesian throughflow water by internal tidal mixing, Geophys. Res. Lett., 34, L04604, doi:10.1029/2006GL028405, 2007.

Koch-Larrouy, A., Atmadipoera, A., Van Beek, P., Madec, G., Aucan, J., Lyard, F., Grelet, J. and Souhaut, M.: Estimates of tidal mixing in the Indonesian archipelago from multidisciplinary INDOMIX in-situ data, Deep Sea Research part 1, M DSR1-D-14-00245R1, in revision, 2015.

Evaluation of an operational ocean model for the Indonesian seas – Part 2

E. Gutknecht et al.

Title Page

Abstract	Introduction
Conclusions	References
Tables	Figures

|◄ | ►|

◄ | ►

| Back | Close |

Full Screen / Esc

Printer-friendly Version

Interactive Discussion

Lehodey, P., Senina, I., and Murtugudde, R.: A spatial ecosystem and populations dynamics model (SEAPODYM) – modeling of tuna and tuna-like populations, Prog. Oceanogr., 78, 304–318, 2008.

Leonard, B. P.: A stable and accurate convective modelling procedure based on quadratic upstream interpolation, Comp. Meth. Appl. M., 19, 59–98, 1979.

Lévy, M., Estublier, A., and Madec, G.: Choice of an advection scheme for biogeochemical models, Geophys. Res. Lett., 28, 3725–3728, 2001.

Ludwig, W., Probst, J. L., and Kempe, S.: Predicting the oceanic input of organic carbon by continental erosion, Global Biogeochem. Cy., 10, 23–41, doi:10.1029/95GB02925, 1996.

Madden, R. A. and Julian, P. R.: Observations of the 40–50 day tropical oscillation – a review, Mon. Weather Rev., 122, 814–837, 1994.

Madec, G.: "NEMO ocean engine", Note du Pole de modélisation, Institut Pierre-Simon Laplace (IPSL), France, No 27 ISSN No 1288–1619, 2008.

Madec, G., Delecluse, P., Imbard, M., and Lévy, C.: OPA 8.1 Ocean General Circulation Model reference manual, Note du Pole de modélisation, Institut Pierre-Simon Laplace (IPSL), France, No11, 91 pp., 1998.

Milliman, J. D., Farnsworth, K. L., and Albertin, C. S.: Flux and fate of fluvial sediments leaving large islands in the East Indies, J. Sea Res., 41, 97–107, 1999.

Moore, T. S., Campbell, J. W., and Dowell, M. D: A class-based approach to characterizing and mapping the uncertainty of the MODIS ocean chlorophyll product, Remote Sens. Environ., 113, 2424–2430, 2009.

Mora, C., Chittaro, P. M., Sale, P. F., Kritzer, J. P., and Ludsin, S. A.: Patterns and processes in reef fish diversity, Nature, 421, 933–936, doi:10.1038/nature01393, 2003.

Moriarty, R. and O'Brien, T. D.: Distribution of mesozooplankton biomass in the global ocean, Earth Syst. Sci. Data, 5, 45–55, doi:10.5194/essd-5-45-2013, 2013.

Pimentel, D., Harvey, C., Resosudarmo, P., Sinclair, K., Kurz, D., McNair, M., Crist, C., Shpritz, L., Fitton, L., Saffouri, R., and Blair, R: Environmental and economic costs of soil erosion and conservation benefits, Science, 267, 1117–1123, 1995.

Rixen, T., Ittekkot, V., Herunadi, B., Wetzel, P., Maier-Reimer, E., and Gaye-Haake, B.: ENSO-driven carbon see saw in the Indo-Pacific, Geophys. Res. Lett., 33, L07606, doi:10.1029/2005GL024965, 2006.

Roberts, C. M., McClean, C. J., Veron, J. E. N., Hawkins, J. P., Allen, G. R., McAllister, D. E., Mittermeier, C. G., Schueler, F. W., Spalding, M., Wells, F., Vynne, C., and Werner, T. B.: Marine

Evaluation of an operational ocean model for the Indonesian seas – Part 2

E. Gutknecht et al.

Title Page

Abstract | Introduction

Conclusions | References

Tables | Figures

◀ | ▶

◀ | ▶

Back | Close

Full Screen / Esc

Printer-friendly Version

Interactive Discussion

biodiversity hotspots and conservation priorities for tropical reefs, Science, 295, 1280–1284, doi:10.1126/science.1067728, 2002.

Romero, O. E., Rixen, T., and Herunadi, B.: Effects of hydrographic and climatic forcing on diatom production and export in the tropical southeastern Indian Ocean, Mar. Ecol.-Prog. Ser., 384, 69–82, doi:10.3354/meps08013, 2009.

Sprintall, J., Gordon, A. L., Murtugudde, R., and Susanto, R. D.: A semi-annual Indian Ocean forced Kelvin waves observed in the Indonesian seas, May 1997, J. Geophys. Res., 105, 17217–17230, doi:10.1029/2000JC900065, 2000.

Susanto, R. D. and Marra, J.: Effect of the 1997/98 El Niño on chlorophyll a variability along the southern coasts of Java and Sumatra, Oceanography, 18, 124–127, doi:10.5670/oceanog.2005.13, 2005.

Susanto, R. D., Gordon, A. L., Sprintall, J., and Herunadi, B.: Intraseasonal variability and tides in Makassar Strait, Geophys. Res. Lett., 27, 1499–1502, 2000.

Susanto, R. D., Gordon, A. L., and Zheng, Q.: Upwelling along the coasts of Java and Sumatra and its relation to ENSO, Geophys. Res. Lett., 28, 1599–1602, doi:10.1029/2000GL011844, 2001.

Susanto, R. D., Moore, T. S., and Marra, J.: Ocean color variability in the Indonesian seas during the SeaWiFS era, Geochem. Geophy. Geosy., 7, Q05021, doi:10.1029/2005GC001009, 2006.

Tranchant, B., Reffray, G., Greiner, E., Nugroho, D., Koch-Larrouy, A., and Gaspar, P.: Evaluation of an operational ocean model configuration at 1/12° spatial resolution for the Indonesian seas – Part 1: Ocean physics, Geosci. Model Dev. Discuss., 8, 6611–6668, doi:10.5194/gmdd-8-6611-2015, 2015.

UNEP: Vantier, L., Wilkinson, C., Lawrence, D., and Souter, D. (Eds.): Indonesian Seas, GIWA Regional Assessment 57, University of Kalmar, Kalmar, Sweden, 2005.

UNEP: Sherman, K. and Hempel, G. (Eds.): The UNEP Large Marine Ecosystem Report: A perspective on changing conditions in LMEs of the world's Regional Seas, United Nations Environment Programme Nairobi, Kenya, 2009.

Van Leer, B.: Towards the ultimate conservative difference scheme. IV. A new approach to numerical convection, J. Comput. Phys., 23, 276–299, 1977.

Veron, J. E. E., Devantier, L. M., Turak, E., Green, A. L., Kininmonth, S., Stafford-Smith, M., and Peterson, N.: Delineating the Coral Triangle, Galaxea, J. Coral Reef Studies, 11, 91–100, 2009.

Title Page

Abstract | Introduction

Conclusions | References

Tables | Figures

◀ | ▶

◀ | ▶

Back | Close

Full Screen / Esc

Printer-friendly Version

Interactive Discussion

Westberry, T., Behrenfeld, M. J., Siegel, D. A., and Boss, E.: Carbon-based primary productivity modeling with vertically resolved photoacclimation, Global Biogeochem. Cy., 22, GB2024, doi:10.1029/2007GB003078, 2008.

WOA: World Ocean Atlas, available at: http://www.nodc.noaa.gov/OC5/WOA09/pr_woa09.html (last access: 13 August 2015), 2009.

WOD: World Ocean Database, available at: http://www.nodc.noaa.gov/OC5/WOD09/pr_wod09.html (last access: 13 August 2015), 2009.

Zalezak, S. T.: Fully multidimensional flux-corrected transport algorithms for fluids, J. Comput. Phys., 31, 335–362, 1979.

Evaluation of an operational ocean model for the Indonesian seas – Part 2

E. Gutknecht et al.

Title Page

Abstract	Introduction
Conclusions	References
Tables	Figures

|◀   ▶|

◀   ▶

Back   Close

Full Screen / Esc

Printer-friendly Version

Interactive Discussion

**Table 1.** Initial and open boundary conditions used for the INDO12BIO configuration.

Variables	Initial Conditions	OBC
NO_3, O_2, PO_4, Si	From WOA Jan[a]	WOA monthly[a]
DIC, ALK	GLODAP annual[b]	GLODAP annual[b]
DCHL, NCHL, PHY2, PHY1	From SeaWiFS Jan[c]	From SeaWiFS monthly[c]
NH_4	Analytical profile[d]	Analytical profile[d]
The others	ORCA2 Jan	ORCA2 monthly

[a] From World Ocean Atlas (WOA 2009) monthly climatology, with increased nutrient concentrations along the coasts (necessary adaptation due to crucial lack of data in the studied area).
[b] Key et al. (2004).
[c] From SeaWiFS monthly climatology. Phytoplankton is deduced using constant ratios of $1.59\,g\,Chl\,mol\,N^{-1}$ and $122/16\,mol\,C\,mol\,N^{-1}$, and exponential decrease with depth.
[d] Low values offshore and increasing concentrations onshore.
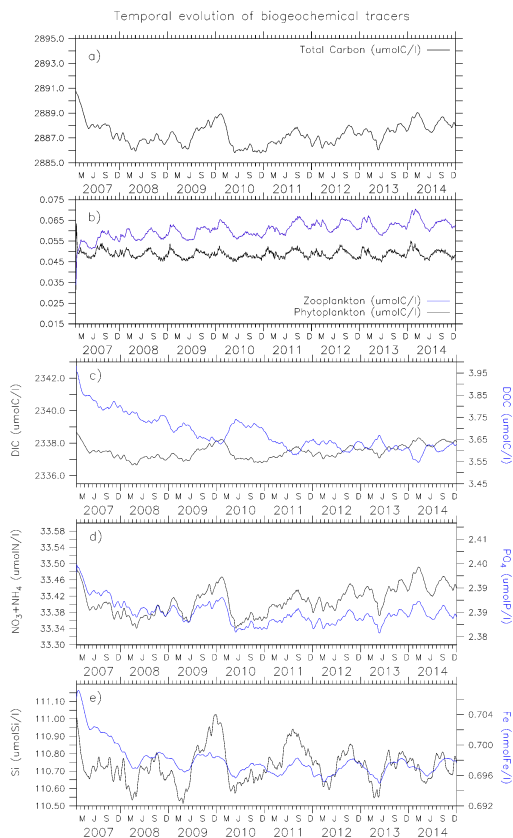
Figure 1. Temporal evolution of total carbon **(a)**, plankton **(b)**, DIC and DOC **(c)** and nutrient **(d, e)** content averaged over the whole 3-dimensional INDO12BIO domain.
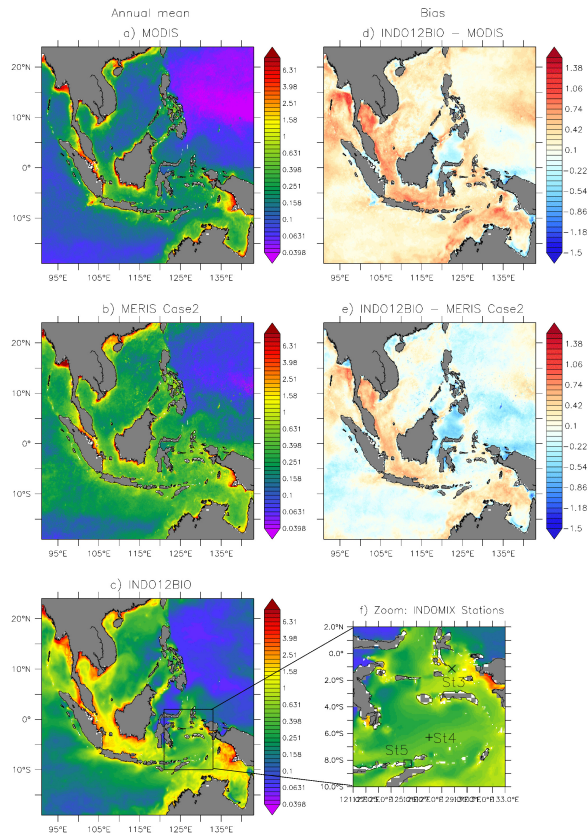
Figure 2. (Left) Annual mean of surface chlorophyll *a* concentrations (mg Chl m^{-3}) for year 2011: MODIS Case 1 product **(a)**, MERIS Case 2 product **(b)** and INDO12BIO simulation **(c)**. (Right) Bias of log-transformed surface chlorophyll (model–observation) for the same year. The model was masked as a function of the observation, MODIS Case 1 **(d)** or MERIS Case 2 **(e)**. Location of 3 stations sampled during the INDOMIX cruise and used for evaluation of the model in Sect. 4.4 **(f)**.
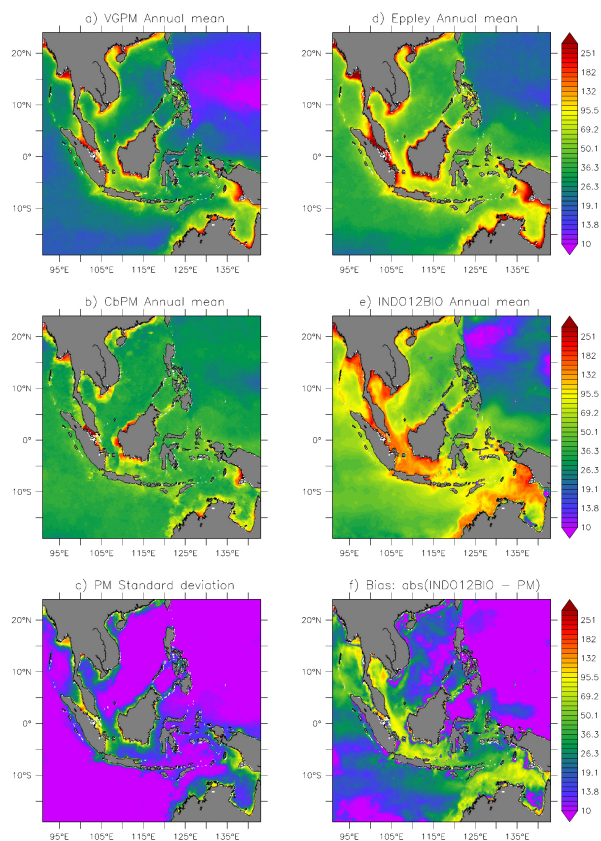
Figure 3. Annual mean of vertically integrated primary production ($mmol\,C\,m^{-2}\,d^{-1}$) for year 2011: VGPM **(a)**, Eppley **(d)**, and CbPM **(b)** production models, all based on MODIS ocean colour, as well as for INDO12BIO **(e)**. Standard deviation of production models (PM) **(c)**, and bias between INDO12BIO and the average of PM **(f)**.

Title Page

Abstract | Introduction

Conclusions | References

Tables | Figures

◀ | ▶

◀ | ▶

Back | Close

Full Screen / Esc

Printer-friendly Version

Interactive Discussion
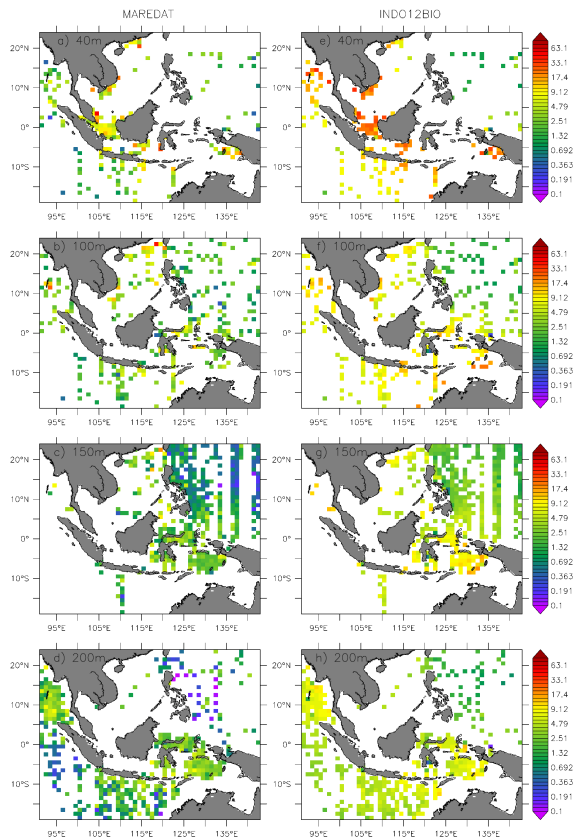
Figure 4. Annual mean of mesozooplankton biomass ($\mu g\,C\,L^{-1}$) from MAREDAT monthly climatology (left) and from INDO12BIO simulation averaged between 2010 and 2014 (right), for distinct depth interval: from the surface up to 40 m **(a, e)**, 100 m **(b, f)**, 150 m **(c, g)**, and 200 m depth **(d, h)**. Simulated fields were interpolated onto the MAREDAT grid, and masked as a function of the data (in space and time).

Full Screen / Esc

Printer-friendly Version

Interactive Discussion
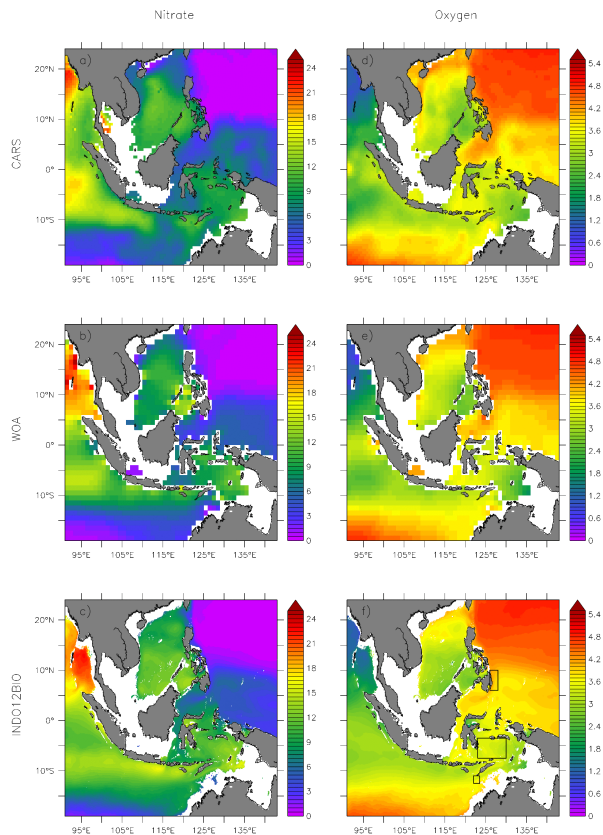
Figure 5. Annual mean of nitrate (mmol N m^{-3}; left) and oxygen concentrations (ml O$_2$ L^{-1}; right) at 100 m depth from CARS **(a, d)** and WOA (**b**, **e**; statistical mean) annual climatologies, and from INDO12BIO as 2010–2014 averages **(c, f)**. Three key boxes for water mass transformation (North Pacific, Banda, and Timor; Koch-Larrouy et al., 2007) were added to the bottom-right figure.

Title Page

Abstract · Introduction

Conclusions · References

Tables · Figures

|◄ · ►|

◄ · ►

Back · Close

Full Screen / Esc

Printer-friendly Version

Interactive Discussion
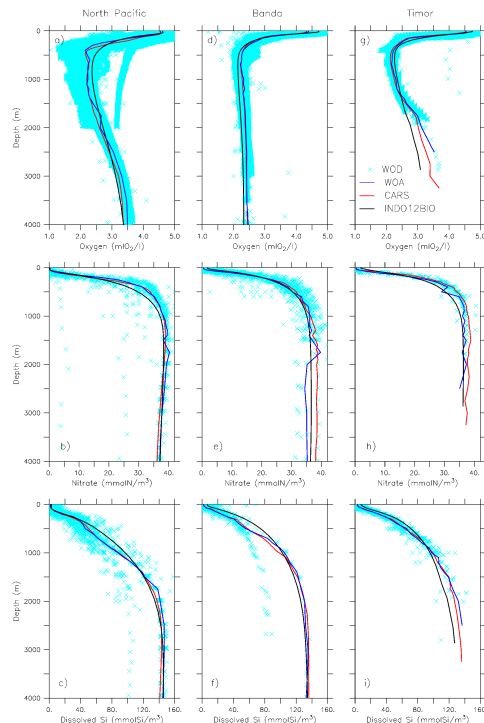
Figure 6. Vertical profiles of oxygen (ml O_2 L^{-1}; top: **a**, **d**, **g**), nitrate (mmol N m^{-3}; middle: **b**, **e**, **h**) and dissolved silica (mmol Si m^{-3}; bottom: **c**, **f**, **i**) in 3 key boxes for water masses transformation (North Pacific, left; Banda, middle; and Timor, right) (see Fig. 5; Koch-Larrouy et al., 2007). CARS and WOA annual climatologies are in red and dark blue. INDO12BIO simulation averaged between 2010 and 2014 is in black. All the raw data available on each box and gathered in the WOD (light blue crosses) are added in order to illustrate the dispersion of data.
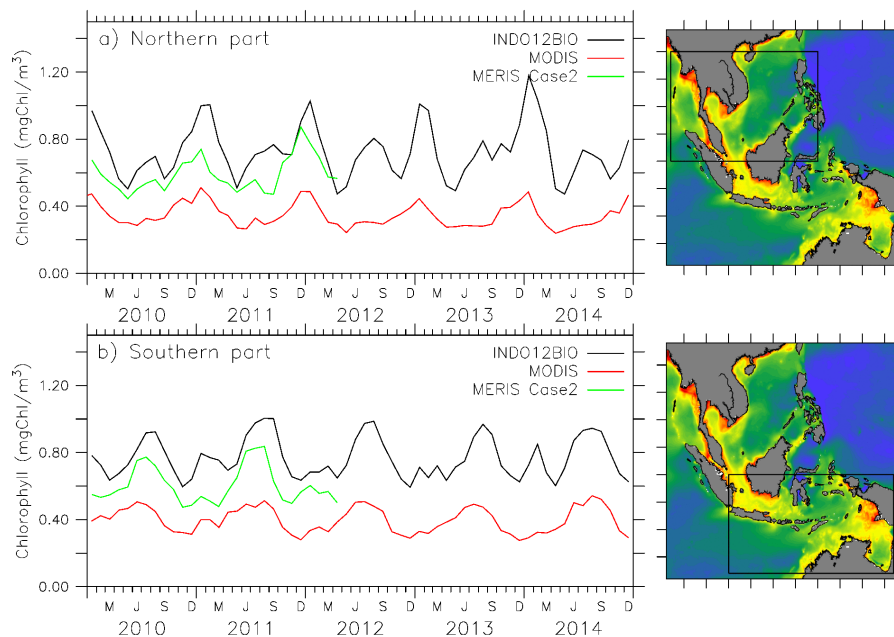
Figure 7. Temporal variation of surface chlorophyll *a* concentrations (mg Chl m^{-3}) averaged over Northern **(a)** and Southern **(b)** parts of the archipelago: INDO12BIO (black), MODIS Case 1 (red) and MERIS Case 2 (green).

Full Screen / Esc
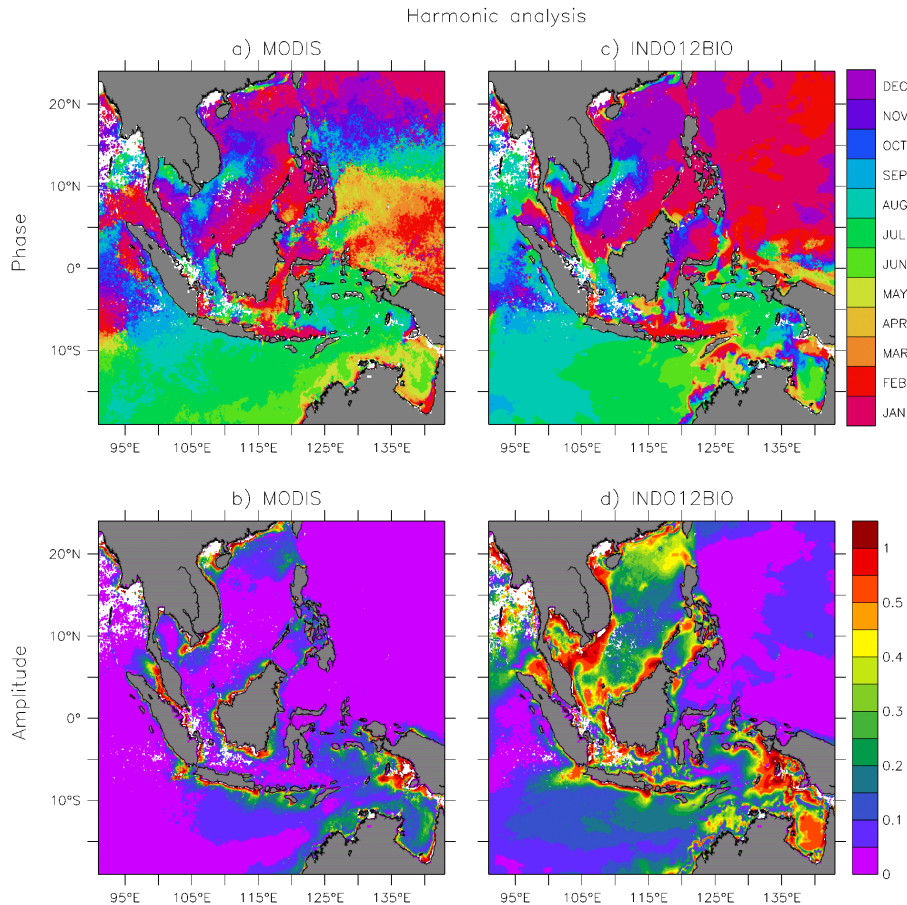
Figure 8. Phase **(a, c)**, and amplitude **(b, d)** of the harmonic analysis computed for a monthly climatology of surface chlorophyll *a* concentrations between 2010 and 2014: MODIS Case 1 (left) and INDO12BIO (right). The model was masked as a function of the data.
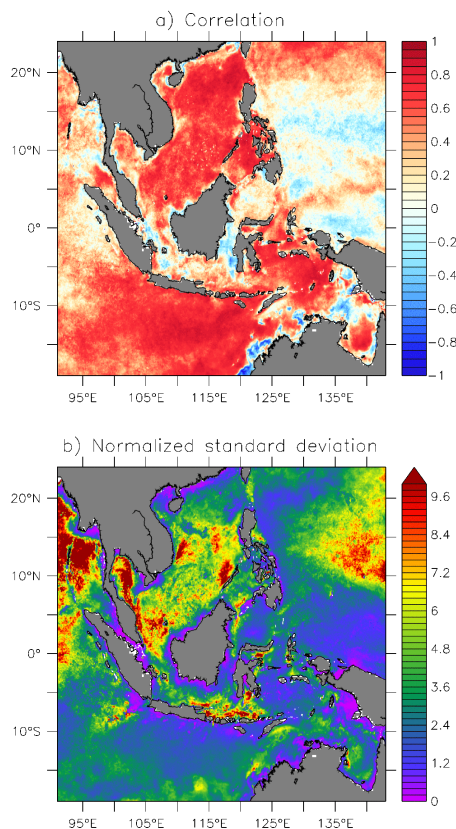
Figure 9. Temporal correlation **(a)** and normalised standard deviation **(b)** estimated between the INDO12BIO simulation and the MODIS Case 1 ocean colour product. Statistics are computed on monthly fields between 2010 and 2014. The model was masked as a function of the data.
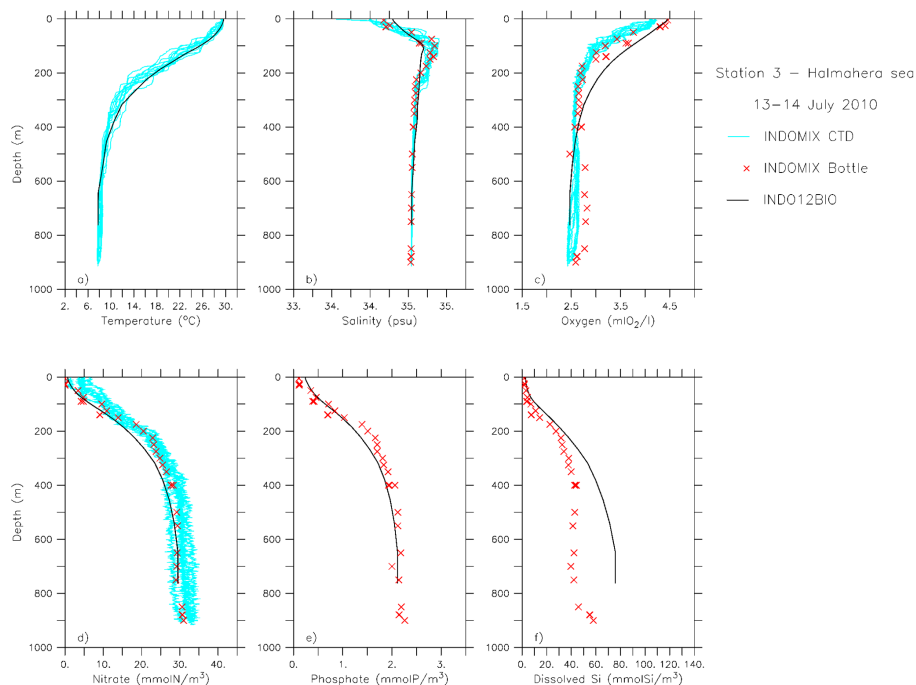
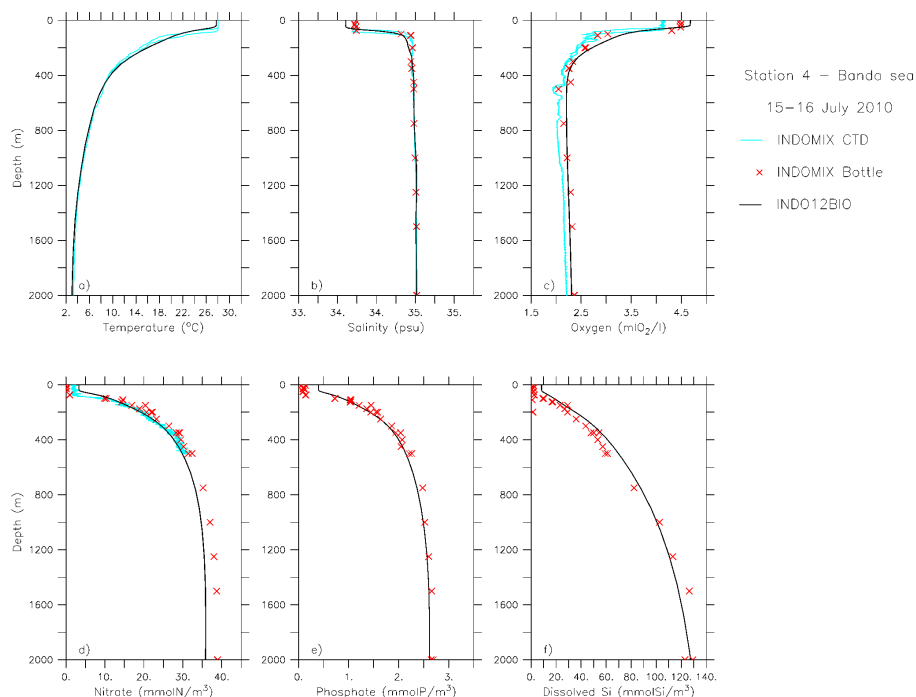**Figure 10.** Vertical profiles of temperature ($^\circ$C; **a**), salinity (psu; **b**), oxygen (ml O_2 L^{-1}; **c**), nitrate (mmol N m^{-3}; **d**), phosphate (mmol P m^{-3}; **e**), and dissolved silica (mmol Si m^{-3}; **f**) concentrations at INDOMIX cruise Station 3 (Halmahera Sea; 13–14 July 2010). CTD (light blue lines) and bottle (red crosses) measurements represent the conditions during cruise, 2 day model averages are shown by the black line.

Figure 11. Vertical profiles of temperature (˚C; **a**), salinity (psu; **b**), oxygen (ml O$_2$ L^{-1}; **c**), nitrate (mmol N m^{-3}; **d**), phosphate (mmol P m^{-3}; **e**), and dissolved silica (mmol Si m^{-3}; **f**) concentrations at INDOMIX cruise Station 4 (Banda Sea; 15–16 July 2010). CTD (light blue lines) and bottle (red crosses) measurements represent the conditions during cruise, 2 day model averages are shown by the black line.

Title Page

Abstract | Introduction

Conclusions | References

Tables | Figures

|◀ | ▶|

◀ | ▶

Back | Close

Full Screen / Esc

Printer-friendly Version

Interactive Discussion
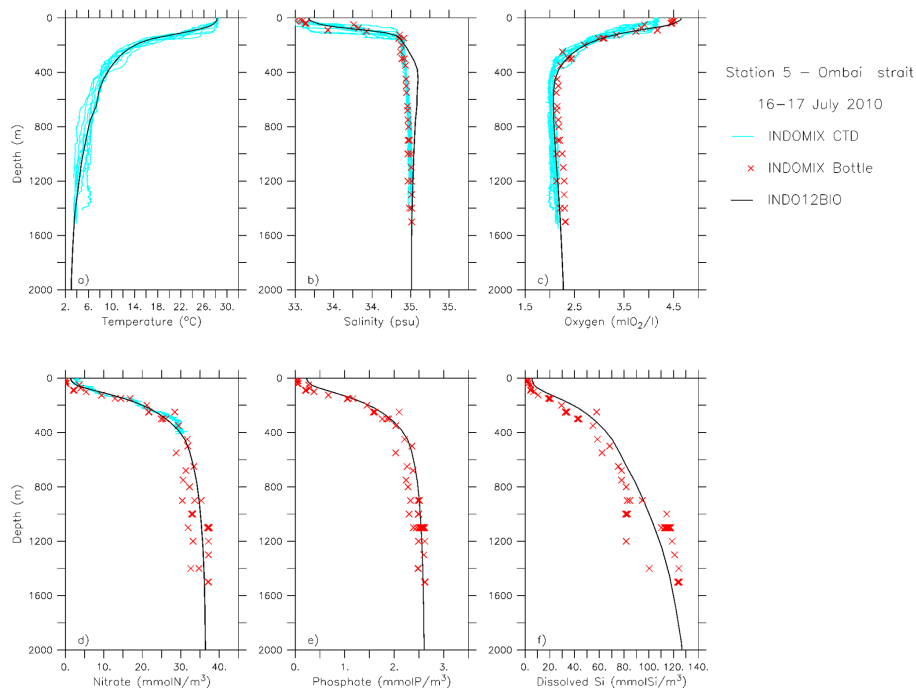
Figure 12. Vertical profiles of temperature (˚C; **a**), salinity (psu; **b**), oxygen (ml O_2 L^{-1}; **c**), nitrate (mmol N m^{-3}; **d**), phosphate (mmol P m^{-3}; **e**), and dissolved silica (mmol Si m^{-3}; **f**) concentrations at INDOMIX cruise Station 5 (Ombaï Strait; 16–17 July 2010). CTD (light blue lines) and bottle (red crosses) measurements represent the conditions during cruise, 2 day model averages are shown by the black line.